3
THE GLOBAL CARBON CYCLE: GEOLOGICAL PROCESSES

Klaus Wallmann[1] and Giovanni Aloisi[1,2]

[1]Leibniz Institute for Marine Sciences (IFM-GEOMAR), Wischhofstrasse, 1–3; 24148, Kiel, Germany
[2]UMR CNRS 7159LOCEAN, Universite Pierre et Marie Curie, Paris, France

3.1 Introduction

In this chapter, we will discuss the geological carbon cycle including all processes controlling the distribution of carbon between the interior of the Earth, the lithosphere, the hydrosphere and the atmosphere (Fig. 3.1, Table 3.1). Our discussion focuses on the geochemical evolution of carbon inventories and fluxes on a multimillion year timescale. We will first address the magnitude of carbon fluxes in the pre-human Holocene and then over the last million years. We next examine the feedbacks stabilizing the distribution of carbon on our planet and present a balanced geological carbon cycle. Subsequently, we explore proxies and models to explain how carbon cycling may have changed over the Earth's geological history in parallel with its biological and geological evolution.

3.2 Organic carbon cycling

Land plants and phytoplankton use solar energy to convert atmospheric CO_2 into biomass via photosynthesis. The overall stoichiometry of photosynthesis can be expressed as:

$$CO_2 + H_2O \Rightarrow C(H_2O) + O_2 \quad (3.1)$$

where the simple carbohydrate $C(H_2O)$ represents organic carbon formed by this process. Molecular oxygen (O_2) is released as an important by-product of this reaction (see Chapter 7). Most of the biomass formed by photosynthesis, however, is rapidly consumed by microorganisms living in soils and in the oceans. Just as humans do, they use the biomass as an energy resource and recycle CO_2 into the atmosphere (electron acceptors other than O_2 are also used to oxidize organic matter as described below):

$$C(H_2O) + O_2 \Rightarrow CO_2 + H_2O \quad (3.2)$$

This respiration process consumes more than 99% of the biomass produced by photosynthesis both on land and in the sea (Table 3.2). On land, the remaining biomass accumulates in living vegetation, soils and detritus, but this is only transient, as most terrestrial organic matter is finally exported into the oceans by rivers in dissolved or particulate form (IPCC, 2007). Overall, approximately 4–5 Tmol yr^{-1} of terrestrial organic matter accumulates in marine sediments deposited on the continental shelf (Burdige, 2005). During certain periods of the geological past (e.g. Permian, Carboniferous) however, the accumulation of terrestrial organic carbon in swamps and wetlands contributed significantly to the global carbon burial flux (Berner and Canfield, 1989).

Ancient marine sediments represented by shales are by far the largest reservoir of organic carbon on our planet. Organic matter is liberated from these rocks, and other rocks including carbonates, by physical erosion and chemical weathering. Even though this old organic matter is much more resistant towards microbial degradation than young organic carbon in soils, studies indicate that it is oxidized by microbes in the presence of atmospheric oxygen (Petsch *et al.*, 2001). Thus, if the oxidation reactions proceed much faster than the geological processes (uplift, physical erosion, chemical weathering) that expose fossil organic matter to the atmosphere

Fundamentals of Geobiology, First Edition. Edited by Andrew H. Knoll, Donald E. Canfield and Kurt O. Konhauser.

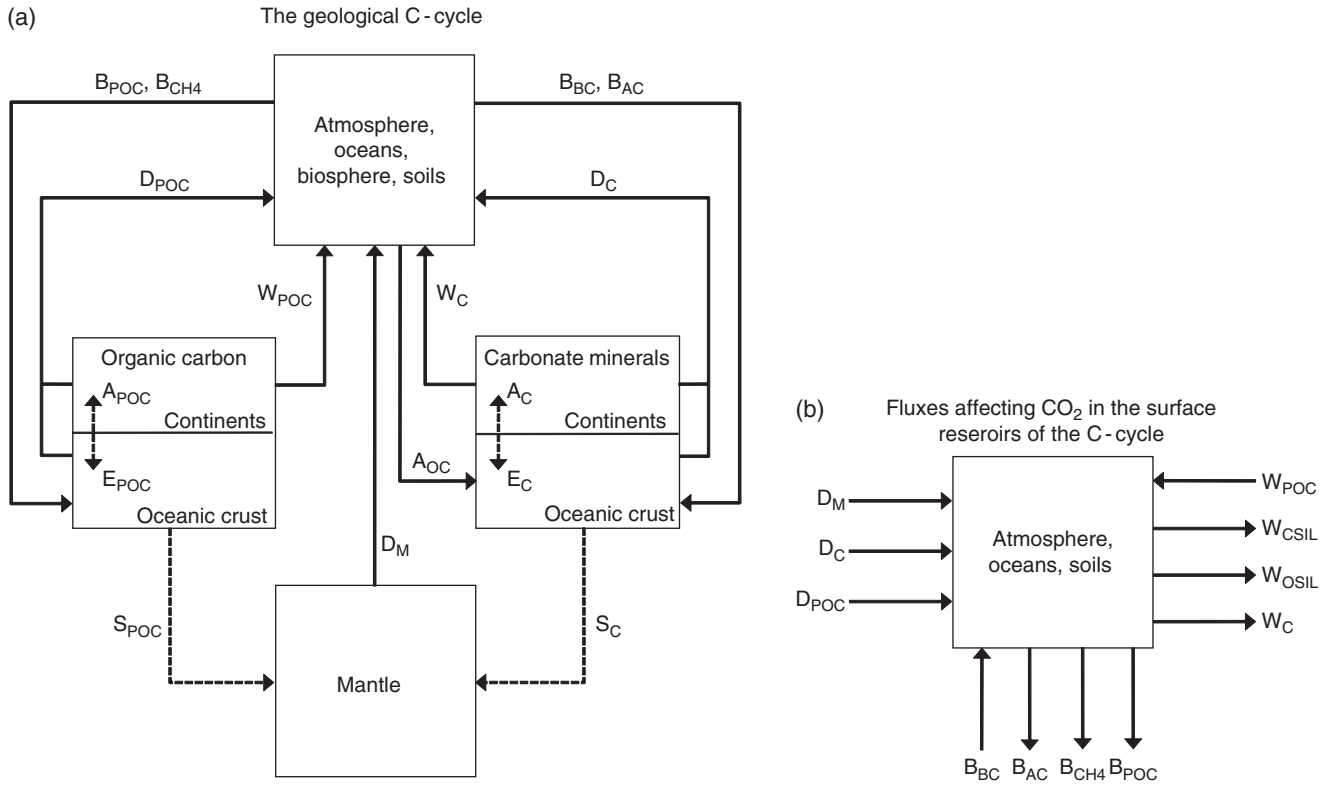

Figure 3.1 (a) The geological carbon (C) cycle; (b) fluxes affecting the concentration of carbon dioxide (CO_2) in the surface reservoir of the carbon cycle. Notes: fluxes that are discussed in detail and quantified in the present work are solid arrows: B_{POC} (burial of POC in marine sediments), B_{CH4} (burial of methane in marine sediments), B_{BC} (burial of biogenic carbonates in marine sediments), B_{AC} (burial of authigenic carbonates in marine sediments), D_{POC} (metamorphic degassing of POC), D_C (metamorphic degassing of carbonate minerals), D_M (degassing of the mantle), W_{POC} (weathering of POC on the continents), W_C (weathering of carbonates on the continents), A_{OC} (alteration of oceanic crust), W_{CSIL} (weathering of silicate minerals on the continents), W_{OSIL} (weathering of silicate minerals in marine sediments). Other carbon fluxes are (dashed arrows): E_{POC} (erosion and transport of POC to the ocean), A_{POC} (accretion of POC during continental collision), E_C (erosion and transport of carbonate minerals to the ocean), A_C (accretion of carbonate minerals during continental collision), S_{POC} (subduction of POC in the mantle), S_C (subduction of carbonate minerals in the mantle).

Table 3.1 Distribution of carbon on our planet (pre-human Holocene)

Substance	Mass (10^{18} mol)
Carbonate C in rocks	5000
Organic C in rocks	1250
Methane in gas hydrates	0.1–0.3
C in soil	0.3
Inorganic C dissolved in deep ocean (>100 m water depth)	2.7
Inorganic C dissolved in upper ocean (0–100 m water depth)	0.1
Atmospheric CO_2	0.06
Terrestrial biosphere	0.05
Marine biosphere	0.0005

Modified from Berner (2004) and Wallmann (2001).

Table 3.2 The global cycle of organic carbon (pre-human Holocene, fluxes in Tmol C yr^{-1})

	Land
CO_2-fixation in living biomass	4700
Accumulation of terrestrial organic carbon in vegetation, soil and detritus	33
Export of terrestrial organic carbon to the oceans	33
Weathering of fossil organic carbon (W_{POC})	8–16
	Oceans
CO_2-fixation in living biomass	4040
Export of marine biomass into the deep ocean	800
Rain of particulate organic matter to the seafloor	190
Burial of organic matter in surface sediments	10–65
Burial of organic matter, authigenic carbonate and methane in deep sediments (B_{POC} + B_{AC} + B_{CH4})	5.4–27

Modified after (IPCC, 2007); (Sarmiento and Gruber, 2006); Burdige, 2007; Wallmann, 2001; Wallmann *et al*., 2008. Note: symbols for fluxes correspond to those appearing in Fig. 3.1.

(Berner, 2004), which is normally true (Bolton *et al*., 2006), then upon exposure, a significant fraction of fossil organic carbon is ultimately degraded into CO_2. The total rate of organic carbon weathering is estimated as ~8 Tmol of particulate organic carbon (POC) yr^{-1}, calculated from a rock denudation rate of 22×10^{15} g yr^{-1} (Berner and Berner, 1996) and an average POC concentration in weathering rocks of 0.45 wt-% (Lasaga and Ohmoto, 2002).

The total rate of physical erosion, however, is larger than the rate of continental denudation since much sediment eroded from upland areas is deposited in lowland areas without reaching the oceans. Thus, only about 10% of the sediments eroded in the United States reaches the oceans, whereas the remaining 90 % is re-deposited on the continents (Berner and Berner, 1996). On the other hand, physical erosion has been greatly accelerated by agriculture and other human land-uses. It is thus very difficult to constrain the modern and pre-human rates of physical erosion and organic matter weathering. Considering the available data on physical erosion and continental sediment recycling (Gaillardet *et al*., 1999b) and the modeling results on POC weathering in shales (Bolton *et al*., 2006), we estimate that about 8–16 Tmol of CO_2 yr^{-1} were produced by POC weathering during the pre-human Holocene.

Phytoplankton living in the surface layer of the oceans contribute significantly to the global primary production, and most of the organic matter produced (typically about 80%) is consumed by microbes and zooplankton within the upper ~ 100 m of the water column (Sarmiento and Gruber, 2006). Of the fraction exported into the deeper ocean as sinking particles (Table 3.2), most is degraded during passage to the seafloor. Furthermore, of the particulate organic matter reaching the seafloor a large proportion is consumed by microbes and other benthic organisms living in the top 10 cm of the sediment column. Only a small fraction of this organic matter is finally preserved into marine sediments accumulating at the deep-sea seafloor. However, much more organic matter is preserved in rapidly depositing shallow shelf sediments and there is a consensus that most marine organic carbon is currently buried in these sediments (Dunne *et al*., 2007; Hedges and Keil, 1995; Middelburg *et al*., 1993). The rate of organic carbon burial in seafloor sediments is only poorly constrained (Burdige, 2007) and falls into the broad range of 10–65 Tmol yr^{-1} (Table 3.2). Estimates generated from marine productivity and particle export data (Dunne *et al*., 2007) are much higher than estimates based on mass balances from sediment data (Hedges and Keil, 1995).

Before final preservation, much organic matter is decomposed by anaerobic microbes, of which sulfate reducers are particularly important (see Chapter 5). These microbes use seawater sulfate as an oxidant and convert sedimentary organic matter into bicarbonate (HCO_3^-):

$$C(H_2O) + \frac{1}{2}SO_4^{2-} \Rightarrow HCO_3^- + \frac{1}{2}H_2S \qquad (3.3)$$

Much of the sulfide (HS^- and H_2S) produced is fixed as pyrite (FeS_2) and other authigenic sulfide minerals. Further down in the sediment column, where sulfate is completely consumed, other microbes transform organic carbon into methane (CH_4) and CO_2:

$$C(H_2O) \Rightarrow \tfrac{1}{2}\,CO_2 + \tfrac{1}{2}\,CH_4 \qquad (3.4)$$

Natural gas hydrates are formed in marine sediments from methane produced in deep sediment layers by the microbial degradation of organic matter. Applying the appropriate kinetic rate laws for the microbial degradation of organic matter in marine sediments (Middelburg, 1989; Wallmann *et al*., 2006), it is estimated that only ~20 ± 10% (~ 2–13 Tmol C yr^{-1}) of the organic matter buried in surface sediments is still preserved after 1 million years of microbial degradation. The major portion of buried organic matter (80 ± 10 %) is, thus, transformed into HCO_3^-, CO_2 and CH_4. These metabolites are either recycled into the ocean or fixed as authigenic carbonate minerals, gas hydrates and natural gas in marine sediments (Dickens, 2003; Wallmann *et al*., 2006; Wallmann *et al*., 2008). The burial flux of authigenic $CaCO_3$ in anoxic marine sediments has been estimated as 3.3–13.3 Tmol yr^{-1} (Wallmann *et al*., 2008) while the accumulation rate of methane and methane hydrates in deep sediments may fall into the range of 0.1–0.6 Tmol yr^{-1} (Dickens, 2003).

When considering long-term climatic change and the geochemical evolution of the Earth on a million year time scale, the most relevant fluxes in the recycling of organic carbon are the weathering of fossil organic carbon on land (8–16 Tmol yr^{-1}) and the burial of organic matter, authigenic carbonates and methane in marine sediments (5.4–27 Tmol yr^{-1}; Table 3.2).

3.3 Carbonate cycling

Most of the carbon residing on the surface of the Earth is bound in carbonate minerals (Table 3.1), and the turnover of these carbonates has a profound effect on geological carbon cycling. Today, carbonates are mostly formed by marine organisms using calcium carbonates ($CaCO_3$, calcite or aragonite) as shell material. The overall stoichiometry of this biogenic calcification can be formulated as:

$$Ca^{2+} + 2HCO_3^- \Rightarrow CaCO_3 + CO_2 + H_2O \qquad (3.5)$$

Biogenic carbonate formation thus serves as a sink for seawater bicarbonate and as a source for atmospheric CO_2 (Table 3.3).

Calcification occurs on shallow and warm continental shelf areas where corals and other organisms produce aragonite and calcite in large scale at an estimated 10 Tmol $CaCO_3$ yr^{-1} (Kleypas, 1997). Due to smaller shelf area and a lower sea-level stand, carbonate accumulation was probably reduced to ~3 Tmol yr^{-1} during the last glacial maximum (Kleypas, 1997). The average $CaCO_3$ accumulation rate on the continental shelf over the last one million years may thus be estimated as 4–7 Tmol yr^{-1}.

Much more biogenic carbonate is formed by calcareous plankton living in the open oceans, and about 40–130 Tmol $CaCO_3$ yr^{-1} of this pelagic carbonate is exported into the deep ocean by sinking particles (Berelson *et al.*, 2007; Dunne *et al.*, 2007). Most of the exported carbonate is, however, dissolved on its way to the seafloor because deep water masses are often undersaturated with respect to aragonite and calcite. Moreover, a large fraction of $CaCO_3$ raining to the seafloor is dissolved within surface sediments by metabolic CO_2 produced during the microbial decomposition of sedimentary organic matter (Archer, 1996). The accumulation of pelagic carbonates in seafloor sediments is thus reduced to 10 Tmol yr^{-1} (Berelson *et al.*, 2007). The accumulation rate of pelagic carbonates has probably changed little through glacial/interglacial climate cycles, and the overall global accumulation rate of biogenic carbonate over the last 1 million years may thus be estimated as 14–17 Tmol yr^{-1}.

Table 3.3 Inorganic carbon cycling (pre-human Holocene, fluxes in Tmol C yr^{-1})

CO_2 sources	
Mantle degassing (D_M)	3.1–5.5
Metamorphism of carbonates (M_C)	2.0–4.0
Biogenic carbonate burial (B_{BC})	20.0
CO_2 sinks	
Silicate weathering on land (W_{CSIL})	10–11
Silicate weathering in marine sediments (W_{OSIL})	3.3–13.3
Carbonate weathering (W_C)	12.3
HCO_3^- sources	
Carbonate weathering (W_C)	24.6
Silicate weathering on land (W_{CSIL})	10 –11
Silicate weathering in marine sediments (W_{OSIL})	3.3–13.3
HCO_3^- sinks	
Biogenic carbonate burial (B_{BC})	40.0
Alteration of oceanic crust (A_{OC})	1.5–2.4

Notes: symbols for fluxes correspond to those appearing in Fig. 3.1; B_{BC} and W_C differ for HCO_3^- and CO_2 because of the 2:1 stoichiometry of these carbon species in carbon precipitation–dissolution processes (Equation 3.9).

Bicarbonate dissolved in seawater is precipitated as carbonates during the reaction of oceanic crust with seawater at moderate temperatures (0–50 °C):

$$\text{basaltic ocean crust} + HCO_3^- \Rightarrow CaCO_3 + \text{altered ocean crust} \quad (3.6)$$

Because protons released from HCO_3^- during carbonate precipitation are mostly consumed by seafloor weathering reactions (Wallmann, 2001), the alteration of ocean crust serves as a sink for seawater bicarbonate but not as source for CO_2. Rates of $CaCO_3$ accumulation in oceanic crust are estimated at 1.5–2.4 Tmol of $CaCO_3$ yr^{-1} (Wallmann, 2001).

Carbonates also accumulate in anoxic marine sediments because large amounts of carbonate alkalinity are formed from organic matter decomposition by microbial sulfate reduction, by the anaerobic oxidation of methane, and by the weathering of silicate minerals (Wallmann *et al.*, 2008). The burial flux of authigenic $CaCO_3$ in anoxic marine sediments has been estimated as 3.3–13.3 Tmol yr^{-1} (Wallmann *et al.*, 2008). This carbon flux contributes significantly to the burial of atmospheric CO_2 in marine sediments and may be regarded as part of the organic carbon burial flux.

Most of the bicarbonate in river water is derived from the weathering and dissolution of carbonates on land. Carbonate weathering serves as an important sink for atmospheric CO_2 and a source of seawater bicarbonate:

$$CaCO_3 + CO_2 + H_2O \Rightarrow Ca^{2+} + 2HCO_3^- \quad (3.7)$$

River chemistry data suggest that 12.3 Tmol of CO_2 yr^{-1} are presently consumed by carbonate weathering (Gaillardet *et al.*, 1999b). This flux is probably not strongly affected by human land use and other anthropogenic effects. During glacial sea-level low-stands, carbonate banks and reefs were exposed to the atmosphere. Some studies suggest that because of this, carbonate weathering was enhanced by 2–6 Tmol CO_2 yr^{-1} during the last glacial maximum (Ludwig *et al.*, 1999; Munhoven, 2002). Other studies (Lerman *et al.*, 2007) conclude that lower temperatures, diminished runoff and expanded ice area would have reduced carbonate weathering by 30%. Overall, the average rate of CO_2 consumption through carbonate weathering over the last 1 million years probably falls in the range of 10–16 Tmol yr^{-1}.

3.4 Mantle degassing

Magma is produced by the partial melting of mantle rocks at spreading centres, subduction zones, and hot spot volcanoes. Carbon is an incompatible element that is strongly enriched in the partial melt and delivered to

the surface environment as lava is extruded. ^{3}He, a primordial isotope stored in the mantle, has a similar solubility in magma as CO_2 and can be used to track and trace volcanic CO_2 emissions. The largest ^{3}He fluxes are found at submarine spreading centres. The global ^{3}He flux within this tectonic setting (1000 mol ^{3}He yr^{-1}) is well constrained (Farley *et al*., 1995), and the molar $CO_2/^3$He ratio in the volcanic volatile phase has been measured in hydrothermal fluids (Resing *et al*., 2004) and a large number of fluid and melt inclusions (Marty and Tolstikhin, 1998). It converges towards a value of 2×10^9 (Resing *et al*., 2004). Applying this ratio and the total ^{3}He flux, the CO_2 emissions at spreading centres become 2 Tmol yr^{-1}.

Unfortunately, it is not possible to derive the global ^{3}He flux at subduction zones from the few reliable ^{3}He flux measurements available. Thus, mantle-CO_2 fluxes have been calculated from estimates for magma production and degree of partial melting in this tectonic setting (Marty and Tolstikhin, 1998). With this approach, the release of mantle-CO_2 at subduction zones is estimated as 0.3–0.5 Tmol yr^{-1} (Marty and Tolstikhin, 1998; Sano and Williams, 1996). Additional CO_2 is also released at subduction zones by the metamorphism of subducted carbonate rocks and fossil organic carbon (see below).
Hot spot and intra-plate volcanoes tap deeper into the mantle, and estimates of CO_2 emissions from these types of volcano, though poorly constrained, fall into the range of 0.8–3 Tmol yr^{-1} (Allard, 1992; Marty and Tolstikhin, 1998). The total rate of CO_2 release from the mantle is thus 3.1–5.5 Tmol CO_2 yr^{-1}.

3.5 Metamorphism

Metamorphism takes place at convergent continental margins where during subduction and associated mountain building, rocks are exposed to high temperatures and pressures. Carbonate and organic matter-bearing rocks may release CO_2 into the atmosphere under these conditions. Indeed, Becker *et al*. (2008) estimated that 0.9 Tmol yr^{-1} of metamorphic CO_2 is emitted into the atmosphere in the Himalayas. This CO_2 comes from carbonate rocks and to a smaller extent from organic carbon exposed to high temperatures (~300 °C) at a depth of ~6 km below the surface.

The $^{13}C/^{12}C$ and $^3He/CO_2$ ratios in volcanic gases emitted at subduction zones indicate that most of the CO_2 comes from subducted carbonates (Sano and Williams, 1996). CO_2 measurements at fumaroles indicate that ~3.3 Tmol CO_2 yr^{-1} is emitted into the atmosphere by metamorphic decarbonation of subducting slabs (Sano and Williams, 1996). Decarbonation is promoted by the infiltration of H_2O-rich fluids into carbonate-bearing rocks. This water is mostly released from the lower oceanic crust or from serpentinite, a water-rich mineral formed by the reaction of upper mantle rocks with seawater. Numerical modeling predicts a global CO_2 flux from subducted carbonates of 0.35–3.12 Tmol yr^{-1} (Gorman *et al*., 2006). Considering contributions from the Himalayas and other major collision zones, the total metamorphic release of CO_2 from carbonate-bearing rocks is estimated as 2 – 4 Tmol CO_2 yr^{-1}. The CO_2 contribution from fossil organic carbon is estimated using the $^{13}C/^{12}C$ ratios measured at CO_2-rich fumorals and hot springs in volcanic arcs (Sano and Williams, 1996) and back-arcs of subduction zones (Seward and Kerrick, 1996) and in the Himalayas (Becker *et al*., 2008). Overall, the metamorphic release of organic matter amounts to 0.4–0.6 Tmol of CO_2 yr^{-1}.

3.6 Silicate weathering

Chemical weathering transforms primary silicate minerals such as feldspars into clays and other particulate and dissolved products. The overall reaction may be represented as:

$$\text{primary silicates} + CO_2 \Rightarrow \text{clays} + \text{dissolved metal cations} + H_4SiO_4 + HCO_3^- \quad (3.8)$$

Dissolved metal cations (Mg^{2+}, Ca^{2+}, Na^+, K^+, ...) and silica (H_4SiO_4) are released during this reaction while CO_2 is transformed into bicarbonate (HCO_3^-). The dissolved products are transported into the oceans through rivers and groundwater discharge. Silicate weathering is the most important sink for atmospheric CO_2 on geological time scales. It removes CO_2 from the atmosphere and increases the dissolved bicarbonate load of the oceans.

Studies of river chemistry indicate that about 11.7 Tmol of atmospheric CO_2 yr^{-1} are presently consumed by silicate weathering (Gaillardet *et al*., 1999b), with young basaltic rocks and tephra the most reactive, contributing ~4.1 Tmol CO_2 yr^{-1} to this global weathering rate (Dessert *et al*., 2003). Silicate weathering is promoted by physical erosion because the reactive surface area of silicate minerals is greatly enhanced by the grinding of rocks into finer particles (Gaillardet *et al*., 1999a). Physical erosion has been increased by human land use since cropland, pasture, and open range export much more particulate material than natural forest and grassland (Berner and Berner, 1996). Humans have increased the sediment transport by global rivers through soil erosion by about 16% {Syvitski, 2005, p. 3949}. Considering these man-made effects on physical erosion, the pre-human rate of silicate weathering is here estimated as 10–11 Tmol CO_2 yr^{-1}.

Silicate weathering is enhanced in soils compared to bare rock. This is because soils have a higher partial pressure of CO_2 due to organic matter decompositions

(Lerman *et al*., 2007) and because plants and microbes release organic chemicals which remove Al^{3+} and other cations from the surface of silicate minerals promoting dissolution (Berner and Berner, 1996). Rates of silicate weathering were, therefore, much lower before the advent of land plants during the Paleozoic (Berner, 2004; see chapter 11).

Most importantly, silicate weathering depends on climate and the variables of temperature, runoff, and pCO_2 (Berner, 1994). The hydrological cycle – including evaporation, precipitation, and runoff – is accelerated under warm surface conditions, while high surface temperatures are usually related to elevated pCO_2 values. This threefold link creates a strong climate sensitivity of silicate weathering. The rate of silicate weathering was probably reduced by 10–40 % during the last glacial maximum by cooler surface temperatures, lower pCO_2, diminished runoff and the sealing of land surfaces by the expansion of continental ice shields (Lerman *et al*., 2007; Munhoven, 2002). Thus, the global rate of silicate weathering averaged over the last 1 million years is probably in the range of 6 – 10 Tmol CO_2 yr^{-1}.

Reactive silicate minerals not weathered on land are ultimately deposited on the seafloor in continental margin sediments, and these minerals are reactive within sediments (Maher *et al*., 2004). Silicate weathering rates are especially high in anoxic sediments rich in labile organic matter. Indeed, most of the metabolic CO_2 produced during organic matter decomposition is converted into HCO_3^- by reaction with feldspars, volcanic ash and other silicate minerals (Wallmann *et al*., 2008). The rate of silicate weathering in marine sediments has been estimated as 5–20 Tmol CO_2 yr^{-1}(Wallmann *et al*., 2008). About one third of the bicarbonate generated by marine weathering is fixed in authigenic carbonates and is treated here as part of the organic carbon cycle as it is ultimately produced by organic matter decomposition. The remaining fraction (3.3–13.3 Tmol of HCO_3^- yr^{-1}) is recycled into the oceans. These new data suggest that the rate of marine silicate weathering may be as high as the rate of continental silicate weathering.

3.7 Feedbacks

Drastic changes in atmospheric pCO_2 and seawater bicarbonate concentration are mitigated by negative feedbacks in the geological carbon cycle. As an example, inorganic carbon is removed from the oceans and atmosphere when levels of atmospheric CO_2 or seawater bicarbonate are too high. Such negative feedbacks also work in the opposite direction, where, for example, depleted inventories of inorganic carbon in the oceans and atmosphere can be restored to pre-depletion levels.

The most important negative feedback on atmospheric pCO_2 is through the temperature sensitivity of terrestrial silicate weathering (see below). If volcanoes deliver high doses of CO_2 to the oceans and atmosphere, the concentrations of CO_2 reach only moderate levels. This is because the removal rate of CO_2 by silicate and carbonate weathering is accelerated due to higher temperatures imparted by the higher CO_2 concentrations (Walker *et al*., 1981). Conversely, with a reduced source of CO_2, atmosphere CO_2 concentrations do not fall too low as the resulting lower temperatures reduce the removal rate of CO_2 by weathering. Therefore, the temperature sensitivity of weathering reactions acts to stabilize atmospheric pCO_2.

Bicarbonate concentrations in the oceans are stabilized by another negative feedback loop. Bicarbonate is mainly removed from the oceans by the burial of biogenic carbonates in sediments (see above). Carbonate burial depends on the saturation state of seawater with respect to calcite and aragonite. With high bicarbonate concentrations in seawater, oceans tend to be oversaturated with respect to these carbonate minerals, increasing the accumulation of carbonate in sediments and stabilizing bicarbonate concentration at a moderate level. The equilibrium reaction representing carbonate precipitation and dissolution within the oceans is shown in Equation 3.9.

$$Ca^{2+} + 2HCO_3^- \Leftrightarrow CaCO_3 + CO_2 + H_2O \qquad (3.9)$$

This reaction equation also demonstrates an additional negative feedback on CO_2 since surplus CO_2 delivered by volcanoes and other sources is removed from the oceans and atmosphere by enhanced carbonate dissolution at the seafloor.

Organic carbon burial in the seafloor is another important CO_2 sink (see above). It is ultimately regulated by the inventory of dissolved phosphate in the oceans since phosphate is the major limiting nutrient for marine productivity on geological timescales. Since organic carbon burial and phosphorus removal are enhanced when oceanic phosphate inventories are high, the phosphate inventory and marine productivity are restored to moderate levels by organic matter burial in a negative feedback loop. Phosphate is delivered to the oceans through chemical weathering on land, and since weathering rates are accelerated at high pCO_2, enhanced phosphate delivery to the oceans and elevated organic matter burial dates are promoted by high pCO_2 levels. Thus, organic matter burial provides a negative feedback for the stabilization of atmospheric pCO_2 values (Wallmann, 2001). The C:P ratio of marine phytoplankton increases at elevated pCO_2 levels (Riebesell *et al*., 2007). Therefore, more organic carbon can be fixed and stored in marine sediments for a given oceanic phosphate inventory

when surplus CO_2 is added to the atmosphere. Together, these negative feedbacks have acted to maintain the carbon inventory of oceans and atmosphere at a moderate level throughout Earth's history.

Positive feedbacks may amplify the effects of natural and anthropogenic perturbations to the carbon cycle and destabilize the carbon inventories in oceans and atmosphere. An example relates to marine productivity and organic carbon burial, with dissolved iron in seawater playing a key role in this feedback loop. Iron is another essential nutrient for marine plankton, limiting marine productivity in many areas of the modern ocean (Sarmiento and Gruber, 2006). Iron is mostly delivered to the oceans as wind-blown dust particles. At low pCO_2 values and surface temperatures, land tends to be drier and winds are stronger, resulting in a larger dust and iron flux to the oceans, which may ultimately increase CO_2 removal via ocean fertilization. Through this chain of processes, low pCO_2 values may be further diminished by enhanced marine productivity and organic carbon burial rates in a positive feedback loop. Fortunately, these positive feedbacks are usually mitigated by more powerful negative feedback loops on geological time scales. Otherwise, life on Earth could not be maintained.

3.8 Balancing the geological carbon cycle

In what follows, we apply a mass balance approach to constrain the fluxes in the geological carbon cycle. Ice core data show that atmospheric pCO_2 has ranged from 190 and 280 µatm over the last 400 kyr (Petit *et al.*, 1999) responding to glacial/interglacial cycles without a significant long-term trend. It may thus be concluded that the carbon cycle reached a pseudo-steady state during the last 1 million years with an average pCO_2 of ~230 µatm overprinted by short term oscillations. This steady state is achieved through negative feedbacks stabilizing the global CO_2 inventory in oceans and atmosphere (see above). The long-term mass balance for CO_2 may thus be formulated as:

$$CO_2 \text{ sinks} = CO_2 \text{ sources} \quad (3.10)$$

with

CO_2 sinks = carbonate weathering (W_C) + silicate weathering on land (W_{CSIL}) + silicate weathering in marine sediments (W_{OSIL}) + burial of POC (B_{POC}), authigenic carbonates (B_{AC}), and methane (B_{CH4}) in marine sediments

CO_2 sources = mantle degassing (D_M) + metamorphic degassing of carbonates (D_C) + metamorphic degassing of POC (D_{POC}) + POC weathering (W_{POC}) + biogenic carbonate burial (B_{BC})

where the symbols for the different fluxes of carbon are the same as those which appear in Fig. 3.1. We also assume that the total carbon inventory of oceans and atmosphere reached a steady state:

$$\text{carbon sinks} = \text{carbon sources} \quad (3.11)$$

with

carbon sinks = biogenic carbonate burial (B_{BC}) + burial of POC (B_{POC}), authigenic carbonates (B_{AC}), and methane (B_{CH4}) in marine sediments + alteration of oceanic crust (A_{OC})

carbon sources = mantle degassing (D_M) + metamorphic degassing of carbonates (D_C) + metamorphic degassing of POC (D_{POC}) + POC weathering (W_{POC}) + carbonate weathering (W_C)

Sediment core data reveal a constant base line for the carbon isotopic composition of biogenic carbonates and seawater over the last one million years (Zachos *et al.*, 2001) overprinted by glacial/interglacial fluctuations (Sarmiento and Gruber, 2006). An isotopic mass balance can thus be defined to further constrain the magnitude of geological carbon fluxes:

$$\delta^{13}C \text{ of carbon sinks} = \delta^{13}C \text{ of carbon sources} \quad (3.12)$$

with

$$\delta^{13}C \text{ of carbon sinks} = \delta^{13}C_{CA} \times (B_{BC} + A_{OC}) + \delta^{13}C_{PA} \times (B_{POC} + B_{AC} + B_{CH4})$$

$$\delta^{13}C \text{ of carbon sources} = \delta^{13}C_M \times D_M + \delta^{13}C_{CW} \times (D_C + W_C) + \delta^{13}C_{PW} \times (D_{POC} + W_{POC})$$

The carbon isotopic compositions of the different carbon sinks and sources are given as (Wallmann, 2001): carbonate minerals accumulating at the seafloor ($\delta^{13}C_{CA}$ = 0 ‰), sedimentary POC accumulating at the seafloor ($\delta^{13}C_{PA}$ = −24 ‰), carbonate minerals subject to weathering and metamorphosis ($\delta^{13}C_{CW}$ = +2 ‰), fossil POC subject to weathering and metamorphosis ($\delta^{13}C_{PW}$ = −26 ‰) and mantle CO_2 ($\delta^{13}C_M$ = −5 ‰).

The isotopic composition of carbonates and POC has changed over time (Fig. 3.2). Thus, the $\delta^{13}C$ values of the input fluxes produced by the weathering and metamorphism of ancient rocks ($\delta^{13}C_{CW}$ and $\delta^{13}C_{PW}$) differ from the modern output fluxes generated by POC and $CaCO_3$ accumulation at the seafloor ($\delta^{13}C_{CA}$ and $\delta^{13}C_{PA}$).

Balanced carbon fluxes can be calculated applying the three mass balance equations for CO_2, carbon, and the isotopic composition of the different carbon sources and sinks considering also the range of fluxes estimated above. Technically speaking, this can be achieved with constrained minimization techniques. The results of this exercise are listed in Table 3.4. They indicate that 7.3 Tmol of CO_2 yr^{-1} are released by mantle degassing and metamorphism while 10.6 Tmol of CO_2 yr^{-1} are consumed by silicate weathering on land and in marine sediments. An additional 4.3 Tmol of CO_2 yr^{-1} are released by the

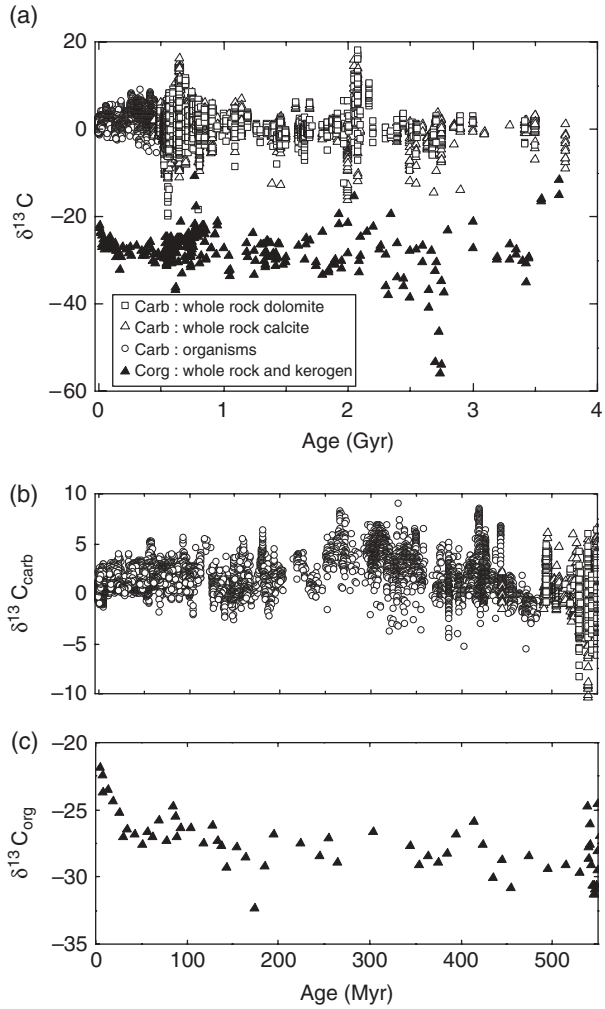

Figure 3.2 $\delta^{13}C_{carb}$ and $\delta^{13}C_{org}$ throughout Earth's history. (a) Complete record for the past 3.8 Gyr. (b) Phanerozoic $\delta^{13}C_{carb}$ record. (c) Phanerozoic $\delta^{13}C_{org}$ record. Note: data from Strauss and Moore (1992), Hayes *et al*. (1999) and Prokoph *et al*. (2008).

turnover of biogenic carbonates (burial – weathering) while 1.0 Tmol of CO_2 yr^{-1} are fixed by POC cycling (burial – weathering). Silicate weathering is, thus consuming volcanic and metamorphic CO_2 and additional CO_2 produced by an imbalance in sedimentary carbon cycling. Seawater bicarbonate is maintained at a steady level by carbonate and silicate weathering adding 23.4 and 10.6 Tmol of HCO_3^- yr^{-1} to the oceans and by the burial of biogenic carbonate and crustal alteration removing 32.0 and 2.0 Tmol of seawater HCO_3^- yr^{-1}. Volcanism is adding mantle carbon into the oceans and atmosphere which is removed by the net growth of the sedimentary carbonate and POC inventories (burial – weathering – metamorphism) and by the alteration of oceanic crust. The residence time of carbon in the oceans and atmosphere is calculated as 102 kyr considering the carbon inventory (2.86×10^6 Tmol of C, Table 3.1) and the balanced input and output fluxes (28.0 Tmol of C yr^{-1}, Table 3.4).

Table 3.4 Mean carbon fluxes over the last 1 million years (in Tmol C yr^{-1})

	Flux Range	Balanced Flux
Carbon sources		
Mantle degassing (D_M)	3.1–5.5	4.3
Metamorphic degassing of carbonate rocks (D_C)	2.0–4.0	2.5
Chemical weathering of carbonate rocks (W_C)	10–16	11.7
Metamorphic degassing of POC (D_{POC})	0.4–0.6	0.5
Chemical weathering of POC (W_{POC})	8–16	9.0
Total		*28.0*
Carbon sinks		
Burial of biogenic carbonate at the seafloor (B_{BC})	14–17	16.0
Alteration of oceanic crust (A_{OC})	1.5–2.4	2.0
Burial of POC, authigenic carbonates, and methane in marine sediments ($B_{POC} + B_{AC} + B_{CH4}$)	5.4–27	10.0
Total		*28.0*
CO_2 sources		
Mantle degassing (D_M)	3.1–5.5	4.3
Metamorphic degassing of carbonate rocks (D_C)	2.0–4.0	2.5
Metamorphic degassing of POC (D_{POC})	0.4–0.6	0.5
Chemical weathering of POC (W_{POC})	8–16	9.0
Burial of biogenic carbonate at the seafloor (B_{BC})	14–17	16.0
Total		*32.3*
CO_2 sinks		
Chemical weathering of silicate rocks on land (W_{CSIL})	6 – 10	7.1
Chemical weathering of silicates in marine sediments (W_{OSIL})	3.3–13.3	3.5
Chemical weathering of carbonate rocks (W_C)	10–16	11.7
Burial of POC, authigenic carbonates, and methane in marine sediments ($W_{POC} + W_{AC} + W_{CH4}$)	5.4–27	10.0
Total		*32.3*

Note: symbols for fluxes correspond to those appearing in Fig. 3.1.

3.9 Evolution of the geological carbon cycle through Earth's history: proxies and models

In what follows, we describe the evolution of the carbon cycle over the past 3.8 Gyr based on available proxy records and results from geochemical models. We begin by discussing the proxy records.

3.9.1 Carbon isotope composition of marine carbonates ($\delta^{13}C_{carb}$) and organic matter ($\delta^{13}C_{org}$)

The stable carbon isotope composition of marine sedimentary carbonates ($\delta^{13}C_{carb}$) provides a record of how the $\delta^{13}C$ of oceanic dissolved inorganic carbon (DIC = $CO_3^{2-} + HCO_3^- + CO_2$) has varied through time. Together with the stable carbon isotope composition of marine sedimentary organic carbon and kerogen ($\delta^{13}C_{org}$), an estimate of the isotopic fractionation accompanying the production and burial of organic carbon ($\varepsilon_{TOC} \approx \delta^{13}C_{carb} - \delta^{13}C_{org}$) can be obtained (Hayes *et al.*, 1999). Of interest to us here is the use of the ε_{TOC} record to estimate the fraction of carbon buried as organic matter in marine sediments (f_o). This provides information on the pace and mechanism of oxidation of the Earth's surface (Hayes and Waldbauer, 2006). In its simplest form, the relation between ε_{TOC} and f_o is:

$$\delta^{13}C_{carb} = \delta^{13}C_{in} + f_o \times \varepsilon_{TOC} \quad (3.13)$$

where $\delta^{13}C_{in}$ is the stable carbon isotopic composition of the carbon input to the surficial system via volcanism, metamorphisms, and continental weathering. This simple relation is valid when the global carbon cycle is in steady state and submarine hydrothermal weathering reactions do not influence the $\delta^{13}C$ of oceanic DIC (Bjerrum and Canfield, 2004; Hayes and Waldbauer, 2006).

Figure 3.2 shows the most recent compilation of $\delta^{13}C_{carb}$ through Earth history (Prokoph *et al.*, 2008) along with a compilation of $\delta^{13}C_{org}$ data obtained by combining a dataset for the last 800 Myr (Hayes *et al.*, 1999) with the Precambrian (540–3800 Myr) dataset of Strauss and Moore (1992). The interested reader can consult the original literature for more information on which type of inorganic and organic phases are analyzed to generate these records and for potential analytical pitfalls.

3.9.2 Strontium isotope composition of marine carbonates ($^{87}Sr/^{86}Sr$)

The $^{87}Sr/^{86}Sr$ ratio in seawater is homogeneous throughout the ocean (Veizer and Compston, 1974). Thus, the $^{87}Sr/^{86}Sr$ ratio as captured in marine carbonates can be used as an indicator of the $^{87}Sr/^{86}Sr$ ratio in ancient seawater. This reflects the relative intensity of the two Sr sources to the ocean: silicate weathering, which releases Sr with high $^{87}Sr/^{86}Sr$ ratios (modern values between 0.705 and 0.735; Gaillardet *et al.*, 1999b), and seafloor spreading, which releases basaltic Sr with low $^{87}Sr/^{86}Sr$ ratios (modern average ~0.703; Teagle *et al.*, 1996). Over long time scales, the evolution of $^{87}Sr/^{86}Sr$ composition of the mantle should also be considered. Thus, mantle $^{87}Sr/^{86}Sr$ increased from ~0.700 at 4.0 Gyr to 0.703 at present due to $^{87}Rb/^{86}Sr$ decay (Shields, 2007). There might also be a temperature-dependent Sr isotope fractionation as Sr is incorporated into carbonate minerals (Fietzke and Eisenhauer, 2006), but this is usually not considered.

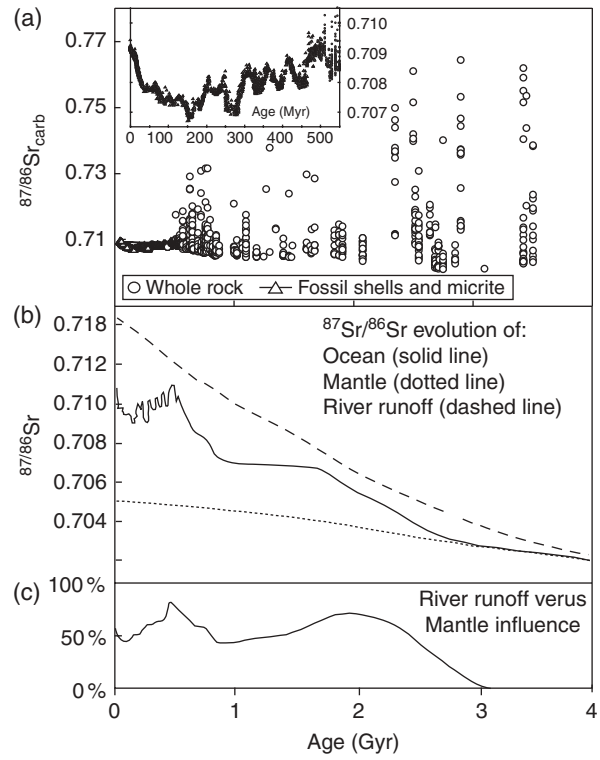

Figure 3.3 $^{87}Sr/^{86}Sr$ evolution of the ocean as an indicator of oceanic crust alteration versus continental weathering inputs of Sr. (a) $^{87}Sr/^{86}Sr$ data throughout the past 3.8 Gyr (Prokoph *et al.*, 2008). Inset: detail of the Phanerozoic $^{87}Sr/^{86}Sr$ record; (b) secular evolution of $^{87}Sr/^{86}Sr$ of the mantle (dotted line), riverine input (dashed line) and ocean (solid line); (c) relative influence of river inputs and ocean crust alteration as Sr sources to the ocean deduced from the curved entry or line in panel (b). Notes: solid line in (b) considers lower envelope of Precambrian $^{87}Sr/^{86}Sr$ values in Prokoph *et al.* (2008); see Shields (2008) for assumptions made to obtain the river runoff curve in panel b; panels (b) and (c) are redrawn from Shields (2008).

Figure 3.3 presents a compilation of $^{87}Sr/^{86}Sr$ of marine carbonates throughout Earth's history (Prokoph *et al.*, 2008). Analyses come from diagenetically unaltered or poorly-altered low-Mg calcite shells of marine organisms (brachiopods, belemnites, corals, inoceramids, planktic foraminifera, oysters) and the apatite shells of conodonts supplemented by whole rock samples to fill stratigraphic gaps in the fossil data and for the Precambrian. While the Phanerozoic record is considered robust, Precambrian $^{87}Sr/^{86}Sr$ values have likely been increased considerably during sedimentary diagenesis (Veizer, 1989).

3.9.3 Proxies of atmospheric pCO_2

Because of the fundamental role of atmospheric CO_2 in regulating climate (Mann *et al.*, 1998; Berner, 2004; Royer

et al., 2007), a number of proxies relating the geochemical characteristics of sediments to past atmospheric CO_2 concentrations have been developed:

1 The $\delta^{13}C$ of pedogenetic minerals (Cerling, 1991). The $\delta^{13}C$ of calcium carbonate or carbonate in goethite formed in soils reflects the relative contribution of biologically produced and atmospherically-derived CO_2, each with distinct $\delta^{13}C$ signatures. With constraints on the contribution from biologically derived CO_2, the $\delta^{13}C$ of pedogenetic minerals can be used to estimate past atmospheric CO_2 concentrations. This technique has been applied to soils from both the Phanerozoic (Ekart *et al*., 1999) and the Precambrian (Rye *et al*., 1995; Sheldon, 2006).

2 The $\delta^{13}C$ of phytoplankton (Freeman and Hayes, 1992). The concentration of dissolved CO_2 is one of the key parameters controlling the carbon isotope difference between the carbon source (dissolved CO_2) and photosynthetically-produced biomass. With careful consideration, the $\Delta^{13}C$ (= $\delta^{13}C_{carb}$ – $\delta^{13}C_{org}$) can be used to reconstruct past atmospheric pCO_2 levels, and this method has been applied to both the Phanerozoic and to certain periods in the Precambrian (Pagani, 1999a, 1999b; Kaufman and Xiao, 2003; Fletcher *et al*., 2005).

3 Stomatal distribution (Van der Burgh *et al*., 1993). In C3 plants, the flux of CO_2 into the leaves is regulated by pores (stomata). Since the abundance of stomata on the leaf epidermis is inversely proportional to pCO_2, the stomatal density of fossil leaves can be used to reconstruct past atmospheric pCO_2 levels. This method provides past pCO_2 estimates in the time interval 0–402 Mya (Rundgren and Beerling, 1999; McElwain and Chaloner, 1995).

4 The $\delta^{11}B$ of planktonic foraminifera (Pearson and Palmer, 2000). The $\delta^{11}B$ of trace boron incorporated in the shells of planktonic foraminifera is thought to reflect that of dissolved $B(OH)_4^-$, one of the two dissolved boron species (the other is $B(OH)_3$). Since the $\delta^{11}B$ of dissolved boron species is a function of seawater pH, the $\delta^{11}B$ of planktonic foraminifera can be used to estimate the pH of surface waters. In conjunction with knowledge of the dissolved inorganic carbon concentration, these estimates are used to calculate atmospheric pCO_2. This method has been applied in the 0–60 Myr time interval.

5 Calcified cyanobacteria (Kah and Riding, 2007). Cyanobacteria – microorganisms with a ≥2.7 Gyr evolutionary history which perform oxygenic photosynthesis – can induce the precipitation of $CaCO_3$ in the cyanobacterial sheath (the matrix of organic molecules which surrounds the cyanobacterial cell). This is thought to occur at low pCO_2 levels, concomitant to the activation of carbon concentrations mechanisms (CCMs), which make HCO_3^- available to cyanobacteria for photosynthesis in CO_2-limited environments. Because CCMs are induced when pCO_2 is lower than 10× the present atmospheric level of CO_2 (PAL) in modern cyanobacteria, the first appearance of calcified cyanobacteria in the sedimentary record (1.2 Gyr) is taken to indicate that atmospheric pCO_2 fell below 10 PAL at that time. This method can be applied only to cyanobacteria that were supposedly calcified in direct contact with bottom ocean waters, rather than in a cyanobacterial mat where chemical conditions differ greatly from those of bottom waters (Aloisi, 2008).

6 Weathering rinds on river gravel (Hessler *et al*., 2004). Pebbles formed 3.2 Gyr ago by continental erosion and river transport of felsic volcanic rocks have an outer layer of altered material (weathering rind) rich in Fe(II) carbonate. Thermodynamic considerations predict that Fe(II) carbonate is the most likely mineral phase to form in this ancient riverine environment if pCO_2 levels are above 2–3 PAL (at lower pCO_2 Fe(II)-layer silicates

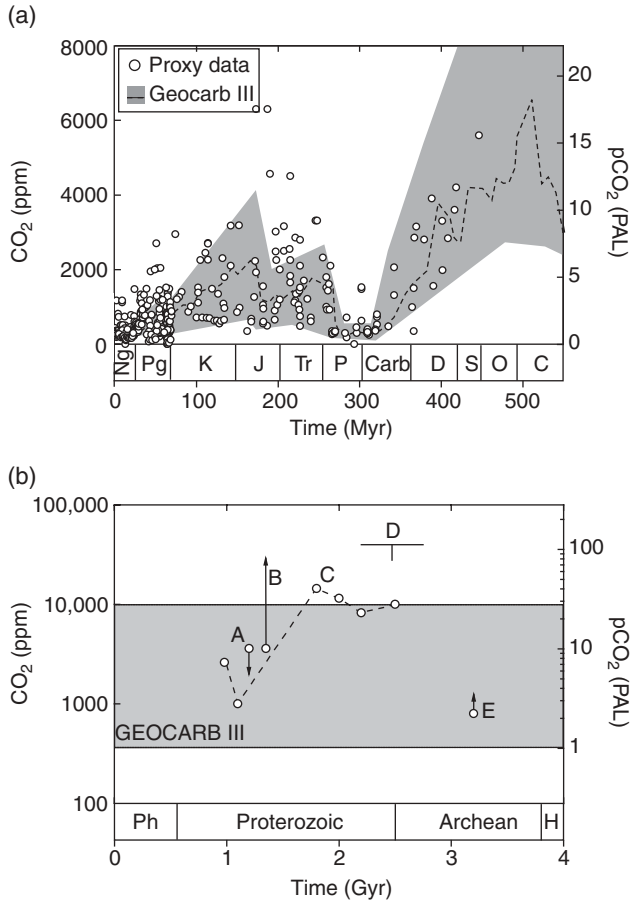

Figure 3.4 Atmospheric pCO_2 throughout Earth's history. (a) Phanerozoic record showing proxy data (circles) and results of the GEOCARB III model. (b) Precambrian proxy data obtained using calcified cyanobacteria (A; Riding and Kah, 2006), acritarchs (B; Kaufman and Xiao, 2003), Paleosols (C,D; Sheldon, 2006 and Rye *et al*., 1995) and weathering rinds (E; Hessler *et al*., 2004).

would form). Thus, atmospheric pCO_2 at 3.2 Gyr must have been ≥2–3 PAL.

Figure 3.4 summarizes the atmospheric pCO_2 proxy data and compares it with Phanerozoic atmospheric pCO_2 estimates obtained with the GEOCARB III model of the global carbon cycle (Berner and Kothavala, 2001).

3.10 The geological C cycle through time

3.10.1 Archean (3.8–2.5 Gyr)

Mantle outgassing and hydrothermal circulation were likely higher in the Archean than today due to a higher thermal flux from the Earth's interior (Sleep and Zahnle, 2001; Lowell and Keller, 2003). The rates of these processes are proportional to the rate of hydrothermal heat flow which can be reconstructed from the thermal characteristics of the oceanic lithosphere and the mantle and the growth history of the continental crust (Lowell and Keller, 2003). Continental growth history, however, is only poorly constrained (Kemp and Hawkesworth, 2005), leading to a great uncertainty of past degassing and hydrothermal circulation rates. One view – the 'big bang' model of continental growth – proposes that continental masses reached their present area very early in Earth's history (<4 Gyr; Armstrong, 1991). Another theory is that the continental growth took place mainly during super-events of crust formation at 2.7, 1.9 and 1.2 Ga (Condie, 1998). Based on an episodic continental growth history where continents grew from 10% to 80% of current area between 3.2 Gyr and 2.5 Gyr (Lowell and Keller, 2003), Hayes and Waldbauer (2006) calculate that the CO_2 degassing flux from the mantle at 3.8 Gs was about nine times higher than today.

With reduced continental surface area and enhanced thermal fluxes, alteration of oceanic crust and basalt carbonation would have probably been the largest CO_2 sink in the Archean (Walker, 1990), accounting for up to 90% of the inorganic carbon removal (Sleep and Zahnle, 2001; Godderis and Veizer, 2000). This removal is evidenced by the widespread presence of hydrothermal carbonates in greenstone belts (Veizer *et al*., 1989; Nakamura and Kato, 2002).

Archean $^{87}Sr/^{86}Sr$ values (Fig. 3.3a) are quite variable ranging from low values of ~0.701 to much higher values of ~0.764. This variability is thought to have resulted from the addition of heavier Sr during sediment diagenesis. Therefore, one typically views the lowest measured values as representative of the $^{87}Sr/^{86}Sr$ of contemporaneous seawater (Prokoph *et al*., 2008). Following this, the ocean had very low $^{87}Sr/^{86}Sr$ values in the Archean. This is partly due to the fact that the $^{87}Sr/^{86}Sr$ of the mantle, which is the ultimate source of Sr to the ocean, has increased though time due to radiogenic decay of ^{87}Rb (Shields, 2007) (Fig. 3.3b). The $^{87}Sr/^{86}Sr$ record, however, departs from the mantle $^{87}Sr/^{86}Sr$ curve around 2.7–2.5 Gyr (Fig. 3.3b) suggesting that at this time the dominant source of Sr to the ocean changed from ocean ridge hydrothermal sources to continental weathering (Shields, 2007; Fig. 3.3c). A general picture emerges which broadly divides Earth's history into pre-Neoarchean times, when the exogenic system was affected principally by inputs from the mantle and post-Neoarchean where mantle fluxes decreased relative to those from continental weathering (Veizer and Compston, 1976; Rey and Coltice, 2008).

The most striking feature of the $\delta^{13}C_{carb}$ and $\delta^{13}C_{org}$ records is, despite some important deviations, the relative constancy of values throughout Earth's history (Fig. 3.2). The $\delta^{13}C$ of carbon released into oceans and atmosphere via mantle degassing, metamorphism and weathering ($\delta^{13}C_{in}$) is usually assumed to have been constant through time and equal to ~–5‰ (Kump and Arthur, 1999; Bjerrum and Canfield, 2004; Hayes and Waldbauer, 2006). Supporting this is the composition of mantle-derived diamonds and carbonatites which have $\delta^{13}C$ ~ –5‰ independent of age of emplacement or location (Kyser, 1986; Mattey, 1987; Pearson *et al*., 2004). When these average $\delta^{13}C$ values are applied to the simplified isotopic mass balance defined in equation 13, it can be concluded that ~20% of carbon was buried in organic form for the past 3.5 Gyr (see, however, Bjerrum and (Canfield, 2004) for a somewhat different view). Hayes and Waldbauer (2006) reconstructed the fraction of carbon buried in the organic form (f_0) and the net accumulation of reduced carbon in the crust in the past 3.8 Gyr using the $\delta^{13}C$ proxies introduced above in conjunction with an isotopic mass balance (similar to Equation 3.13, above) and assumptions on the history of mantle degassing and crust-mantle carbon exchanges (Fig. 3.5). These results seem to indicate that the Archean sedimentary record carries the geochemical imprint of biological carbon cycling operating in an astonishingly stable mode.

The Archean isotope records ends with a prominent negative $\delta^{13}C_{org}$ excursion ($\delta^{13}C_{org}$ down to –60‰) between 2.8 and 2.6 Gyr (Fig. 3.2). Three possible scenarios have been proposed to explain this event:

1 High ^{13}C depletions caused by high rates of methane oxidation by aerobic methanotrophic bacteria and the incorporation of strongly ^{13}C depleted bacterial biomass into the organic carbon pool. The strongly ^{13}C-depleted biomass is produced as methanotrophs oxidize highly ^{13}C depleted methane (Hayes, 1994).

2 Sulfate, instead of oxygen, was used to oxidize methane anaerobically by a microbial consortium of sulfate-reducing bacteria and methanotrophic *Archaea* (Hinrichs, 2002).

3 The ^{13}C-depleted organic matter originated as organic particles formed from a ^{13}C-depleted organic haze in the

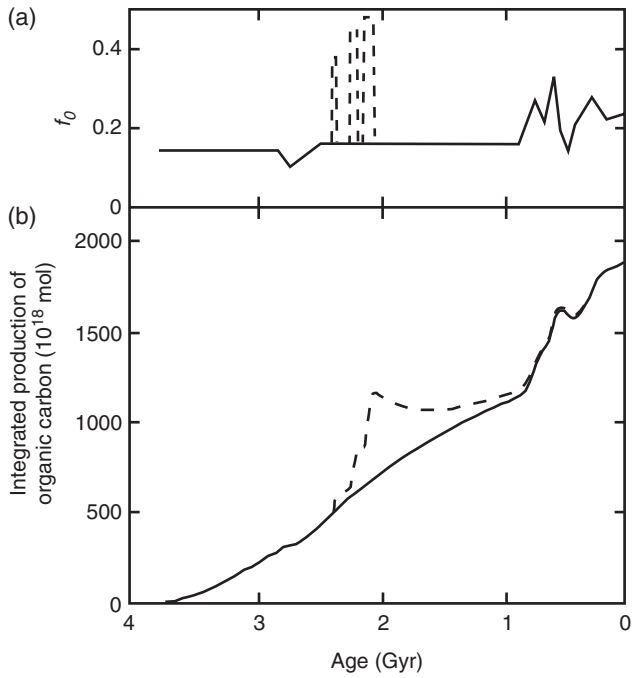

Figure 3.5 Integrated net production of organic carbon, equivalent to the net release of oxidizing power (Emol O_2), in the past 3.8 Gyr (from Hayes and Waldbauer (2006)). (a) estimated values of f_0, the portion of carbon buried in the organic form compared to total buried carbon in the past 3.8 Gyr; (b) Integrated production of organic carbon. Notes: dotted lines consider that the extreme ^{13}C-enrichement of carbonates between 2.3 and 2.0 Gyr reflects a global signal of the ocean (this idea is now considered unlikely, see Hayes and Waldbauer, 2006).

atmosphere. Modeling suggests that such a haze would form when atmospheric $CH_4/CO_2 \geq 1$ (Pavlov *et al*., 2001). A methane-rich Archean atmosphere, and its associated greenhouse warming, is consistent with an emerging view that Archean atmospheric levels where not as high as once thought.

3.10.2 Proterozoic (2.5 Ga–540 Ma)

The Proterozoic $\delta^{13}C_{carb}$ record starts with one of the most controversial excursions of the Precambrian: a globally expressed positive $\delta^{13}C$ excursion of up to 12‰ between 2.3 and 2.0 Ga (Karhu and Holland, 1996; Melezhik *et al*., 1999). Similar enrichments occur also in the 2.44–2.30 Ga and 1.92 – 1.97 Ga intervals but it is not known if these are global events (Melezhik *et al*., 1999). These were initially interpreted as reflecting a nearly threefold increase in the fraction of carbon buried as organic matter (Karhu and Holland, 1996), with a corresponding huge increase in the net release of oxidizing power with consequences for the accumulation of O_2 in the atmosphere (the 'great oxidation event'; Karhu and Holland, 1996; see dotted lines in Fig. 3.5). But a parallel increase in the $\delta^{13}C_{org}$ signal – which would result from primary producers using the ^{13}C-enriched DIC pool – has not been observed; nor have the large organic matter deposits that would result from increased production (Hayes and Waldbauer, 2006). Furthermore, such high levels of primary productivity require unlikely high supplies of phosphate to the ocean (Aharon, 2005).

In another explanation, ^{13}C-enriched carbonates can also be produced in methanogenic sediments, where fermentative processes add ^{13}C-enriched CO_2 to pore waters (Claypool and Kaplan, 1974; Hayes and Waldbauer, 2006). Such diagenetic carbonates are known to occur in modern settings where methanogenesis is intense (Matsumoto, 1989). The methane produced is ^{13}C-depleted (−60 to −100‰) and could be the source of the ^{13}C-depleted inorganic carbon and carbonates where methane is oxidized anaerobically in conjunction with sulfate reduction (Aloisi *et al*., 2002) or aerobically with oxygen, perhaps explaining some the early Proterozoic ^{13}C-depleted carbonates. Should a diagenetic origin of the ^{13}C-rich carbonates be confirmed, it would mean that the ^{13}C-enriched carbonates from the early Proterozoic do not necessarily imply an increase in organic carbon burial and exceptional rates of oxygen production at this time (Fig. 3.5b, solid line as opposed to dashed line).

In the period from 1.8 to 1.3 Gyr, there is little change in the $\delta^{13}C$ of organic or inorganic carbon (Fig. 3.2). This could be due to stability in crustal dynamics, climate and oxidation state of the surface environment (Buick *et al*., 1995; Braiser and Lindsay, 1998) or high oceanic DIC, which would buffer oceanic $\delta^{13}C$ with respect to changes in the carbon inputs to and outputs from the ocean (Bartley and Kah, 2004). From 1.3 Gyr to the Precambrian–Cambrian boundary (540 Myr), the variability in $\delta^{13}C_{carb}$ becomes extreme, with values ranging from −12 to 8‰ between 750 and 600 Myr (Halverson *et al*., 2005). The events driving these extreme $\delta^{13}C$ shifts may have been truly exceptional.

The most extreme isotope variations are partly coincident with global 'snowball Earth' glaciations (Knoll, 1991). Both isotopic discrimination (ε_{TOC}) and the fraction of carbon buried in the organic form (f_0) are high just prior to the Sturtian (between 750 and 700 Myr) and Marinoan (between 663 and 636 Myr) glaciations (Halverson *et al*., 2005).Very positive $\delta^{13}C$ carbonate values occur at the onset of global glaciations followed by negative $\delta^{13}C$ carbonate values during these global ice ages (Kaufman and Knoll, 1995). The most negative values are recorded in post-glacial 'cap' carbonates covering the glaciogenic deposits and during the so-called Shuram–Wonoka anomaly at around 580 to 550 Ma (Fike *et al*., 2006). Rothman *et al*. (2003) have argued that these large negative isotope excursions resulted from the periodic partial oxidation of a huge Neoproterozoic marine DOC pool.

3.10.3 Phanerozoic

During most of the Cambrian to Devonian, pCO_2 values were higher than today (Berner, 1997, 2004, 2006; Farkaš *et al.*, 2007; Wallmann, 2004), likely in the range of 1000–8000 µatm (Royer, 2006; Royer *et al.*, 2007) (Fig. 3.4). These high levels were probably caused by reduced rates of silicate weathering on land. In part, high CO_2 was a consequence of lower solar luminosity. Quite simply, with a less luminous Sun, higher CO_2 concentrations are necessary to raise the Earth surface temperature to the point for sufficient CO_2 removal by weathering. Also, this time was before the advent of land plants and their enhancement of silicate weathering through rooting activity leading to soil formation, enhanced rates organic matter decay, and elevated soil pCO_2 concentrations as discussed above.

A major dip in pCO_2 occurred during the Carboniferous and Permian. The rise and spread of land plants over this period is the ultimate reason for this prominent reduction in pCO_2 (Berner, 1997). As just mentioned, vascular plants greatly promoted soil formation and the consumption of CO_2 via silicate weathering. Extensive burial of organic carbon in wetlands and swamps also added to the dramatic draw-down in pCO_2. Enhanced organic carbon burial is clearly documented by the very positive marine $\delta^{13}C$ values (Fig. 3.2) indicating the pronounced sequestration of ^{12}C in organic matter.

Atmospheric pCO_2 values recovered and reached a maximum during the Jurassic and Cretaceous. These elevated pCO_2 values, ranging between 500 and 4000 µatm, were probably related to enhanced rates of mantle degassing and volcanism. The $^{87}Sr/^{86}Sr$ of marine waters reached a prominent minimum during this period. This indicates high rates of hydrothermal activity at mid-ocean ridges (Fig. 3.3), which correlates with the high rates of seafloor spreading and mantle degassing of CO_2 (Farkaš *et al.*, 2007; Wallmann, 2004).

Over the last ~40 million years, pCO_2 values declined towards the very low Pleistocene to Holocene value of ~230 µatm. This decline was probably caused by enhanced rates of silicate weathering. The collision of India with Asia formed the Himalayas and the Tibetan Plateau increased the rate of physical erosion and CO_2 removal by silicate weathering (Gaillardet *et al.*, 1999b; Raymo, 1994). The marine $^{87}Sr/^{86}Sr$ record supports this scenario. It shows a very rapid increase in $^{87}Sr/^{86}Sr$ over the late Cenozoic indicating that Sr with very high continental-like ratios was released into the oceans (Wallmann, 2001).

During the Anthropocene, pCO_2 values may increase towards a value of ~1000 µatm due mainly to the burning of fossil fuel. Prior to the onset of industrialization, ~10.5 Tmol of CO_2 yr^{-1} were released by POC weathering and metamorphism (Table 3.4). Burning of fossil fuel increased the release of CO_2 from fossil organic carbon by almost two orders of magnitude to >600 Tmol of CO_2 yr^{-1} (IPCC, 2007). CO_2 from fossil organic sources is strongly depleted in the heavy ^{13}C isotope. Thus, the isotopic composition of the atmosphere and the surface ocean has shifted towards more negative $\delta^{13}C$ values due to anthropogenic CO_2 emissions. Models predict that anthropogenic CO_2 will be removed from the atmosphere and taken up by the oceans within the next ~ 100 kyr (Ridgwell and Hargreaves, 2007). The future geological record will thus document the Anthropocene as a sharp negative excursion in the $\delta^{13}C$ of carbonates and organic biomarkers.

3.11 Limitations and perspectives

The geological carbon cycle considers the long-term distribution of carbon on our planet. Thus, most short-term biological fluxes are not considered in the geological carbon cycle as they have rather little effect on the long-term evolution of the major carbon inventories. These are explored in Chapter 2.

A number of important physical processes are typically neglected by most researchers working on global carbon cycling. Thus, the dissolution of atmospheric CO_2 in the oceans, the transport of dissolved carbon compounds by ocean currents, and the out-gassing of oceanic CO_2 into the atmosphere are usually not resolved in long-term carbon cycle models. It is usually assumed that the carbon distribution between the oceans and atmosphere attains equilibrium within less than one million years. While this assumption is basically correct, it may not be strictly valid for ancient oceans with higher inventories of DIC or supporting much lower rates of biological activity.

Motivated by these problems and further important limitations arising in the traditional geological approach, a new generation of geobiologists are coordinating with scientists from other fields such as physical and biological oceanography and climatology to develop new Earth system models resolving the complex interactions between biological, physical, chemical, and geological processes. These ultimately control the pCO_2 of ancient and future atmospheres, seawater pH and the distribution of carbon on our planet.

References

Aharon P (2005) Redox stratification and anoxia of the early Precambrian oceans: implications for carbon isotope excursions and oxidation events. *Precambrian Research* **137**, 207–222.

Allard P (1992) Global emissions of helium-3 by subaereal volcanism. *Geophysical Research Letters* **19**(4), 1479–1481.

Aloisi G (2008) The calcium carbonate saturation state in cyanobacterial mats throughout Earth's history. *Geochimica et Cosmochimica Acta* **72**(24), 6037–6060.

Aloisi G, Bouloubassi I, Heijs SK, *et al.* (2002) CH_4-consuming microorganisms and the formation of carbonate crusts at cold seeps. *Earth and Planetary Science Letters* **203**(1), 195–203.

Archer D (1996) A data-driven model of the global calcite lysocline. *Global Biogeochemical Cycles* **10**(3), 511–526.

Armstrong RL (1991) The persistent myth of crustal growth. *Australian Journal of Earth Sciences* **38(5)**, 613–630.

Bartley JK, Kah LC (2004) Marine carbon reservoir, C_{org}–C_{carb} coupling, and the evolution of the Proterozoic carbon cycle. *Geology* **32**(2), 129–132.

Becker JA, Bickle MJ, Galy A, Holland TJB (2008) Himalayan metamorphic CO_2 fluxes: quantitative constrains from hydrothermal springs. *Earth and Planetarian Science Letters* **265**, 616–629.

Berelson WE, Balch WM, Najjar R, Feely RA, Sabine C, Lee K (2007) Relating estimates of $CaCO_3$ production, export, and dissolution in the water column to measurements of $CaCO_3$ rain into sediment traps and dissolution on the sea floor: a revised global carbonate budget. *Global Biogeochemical Cycles* **21**(GB1024).

Berner RA (1994) GEOCARB II: a revised model of atmospheric CO_2 over Phanerozoic time. *American Journal of Science* **294**, 56–91.

Berner RA (1997) The rise of plants and their effect on weathering and atmospheric CO_2. *Science* **276**, 544–546.

Berner RA (2004) *The Phanerozoic Carbon Cycle: CO_2 and O_2*. Oxford University Press, Oxford.

Berner RA (2006) GEOCARBSULF: a combined model for Phanerozoic atmospheric O_2 and CO_2. *Geochimica et Cosmochimica Acta* **70**, 5653–5664.

Berner EK, Berner RA (1996) *Global Environment: Water, Air and Geochemical Cycles*. Prentice Hall, Englewood Cliffs, NJ.

Berner RA, Canfield DE (1989) A new model for atmospheric oxygen over Phanerozoic time. *American Journal of Science* **289**, 333–361.

Berner RA, Kothavala Z (2001) GEOCARB III: a revised model of atmospheric CO_2 over Phanerozoic time. *American Journal of Science* **301**, 182–204.

Bjerrum CJ, Canfield DE (2004) New insights into the burial history of organic carbon on the early Earth. *Geochemistry, Geophysics, Geosystems* **5**(8), doi:10.1029/2004GC000713.

Bolton EW, Berner RA, Petsch ST (2006) The weathering of sedimentary organic matter as a control on atmospheric O_2: II. Theoretical modeling. *American Journal of Science* **306**, 575–615.

Bowring SA, Housh T (1995) The Earth's early evolution. *Science*, **269**, 1535–1540.

Braiser MD, Lindsay JF (1998) A billion years of environmental stability and the emergence of eukaryotes: new data from northern Australia. *Geology* **23**, 555–558.

Buick R, Des Marais DJ, Knoll AH (1995) Stable isotopic compositions of carbonates from the Mesoproterozoic Bangemall Group, northwestern Australia. *Chemical Geology* **123**, 153–171.

Burdige DJ (2005) Burial of terrestrial organic matter in marine sediments: a re-assessment. *Global Biogeochemical Cycles* **19**(GB4011), doi:10.1029/2004GB002368.

Burdige DA (2007) Preservation of organic matter in marine sediments: controls, mechanisms, and an imbalance in sediment organic carbon budgets? *Chemistry Reviews* **107**, 467–485.

Claypool GE, Kaplan IR (1974) The origin and distribution of methane in marine sediments. In: *Natural Gases in Marine Sediments* (ed Kaplan IR). Plenum, New York, pp. 99–139.

Condie KC (1998) Episodic continental growth and super-continents: a mantle avalanche connection? *Earth and Planetary Science Letters* **163**, 97–108.

Dickens GR (2003) Rethinking the global carbon cycle with a large dynamic and microbially mediated gas hydrate capacitor. *Earth and Planetary Science Letters* **213**, 169–183.

Dunne JP, Sarmiento JL, Gnanadesikan A (2007) A synthesis of global particle export from the surface ocean and cycling through the ocean interior and on the seafloor. *Global Biogeochemical Cycles* **21**(GB4006), doi:10.1029/2006GB002907.

Ekart DD, Cerling TE, Montanez IP, Tabor NJ (1999) A 400 million year carbon isotope record of pedogenetic carbonate; implications for paleoatmospheric carbon dioxide. *American Journal of Science* **299**, 805–827.

Farkaš J, Böhm F, Wallmann K, *et al*. (2007) Calcium isotope budget of Phanerozoic oceans: implications for chemical evolution of seawater and its causative mechanism. *Geochimica et Cosmochimica Acta* **71**, 5117–5134.

Farley KA, Maier-Reimer E, Schlosser P, Broecker WS (1995) Constraints on mantle ^{3}He fluxes and deep-sea circulation from an oceanic general circulation model. *Journal of Geophysical Research* **100**(B3), 3829–3939.

Fietzke J, Eisenhauer A (2006) Determination of the temperature-dependent stable strontium isotope (Sr-88/Sr-86) fractionation via braketing standard MC-ICP-MS. *Geochemistry, Geophysics, Geosystems*, **7**, Q08009, doi:10.1029/2006GC001243.

Fike DA, Grotzinger JP, Pratt LM, *et al*. (2006) Oxidation of the Ediacaran Ocean. *Nature*, **444**, 744–747.

Fletcher BJ, Beerling DJ, Brentnall SJ (2005) Fossil bryophytes as recorders of ancient CO_2 levels: experimental evidence and a Cretaceous case study. *Global Biogeochemical Cycles* **19**, GB3012, doi:10.1029/2005GB002495.

Freeman KH, Hayes JM (1992) Fractionation of carbon isotopes by phytoplankton and estimates of ancient CO_2 levels. *Global Biogeochemical Cycles* **6**, 185–198.

Gaillardet J, Dupré B, Allègre CJ (1999a) Geochemistry of large river suspended sediments: Silicate weathering or recycling tracer. *Geochimica et Cosmochimica Acta* **63**(23/24), 4037–4051.

Gaillardet J, Dupré B, Louvat P, Allègre CJ (1999b) Global silicate weathering and CO_2 consumption rates deduced from the chemistry of large rivers. *Chemical Geology* **159**, 3–30.

Godderis Y, Veizer J (2000) Tectonic control of chemical and isotopic composition of ancient oceans: the impact of continental growth. *American Journal of Science* **300**, 434–461.

Gorman PJ, Kerrick DM, Connolly JAD (2006) Modeling open system metamorphisc decarbonation of subducting slaps. *Geochemistry, Geophysics, Geosystems* **7**(4), Q4007, doi:10.1029/2005GC001125.

Halverson GP, Hoffman PF, Schrag DP, Maloof AC, Rice AHN (2005) Toward a Neoproterozoic composite carbon-isotope record. *GSA Bulletin* **117**(9/10), 1181–1207.

Hayes JM (1994) Global mathanotrophy at the Archean–Proterozoic transition. In: *Early Life on Earth* (ed Bengston S). Nobel Symposium 84, Columbia University Press, New York, pp. 220–236.

Hayes JM, Waldbauer JR (2006) The carbon cycle and associated redox processes through time. *Philosophical Transactions of the Royal Society B* **361**, 931–950.

Hayes JM, Strauss H, Kaufman AJ (1999) The abundance of ^{13}C in marine organic matter and isotopic fractionation in the

global biogeochemical cycle of carbon during the past 800 Ma. *Chemical Geology* **161**, 103–125.

Hedges JI, Keil RG (1995) Sedimentary organic matter preservation: an assessment and speculative synthesis. *Marine Chemistry* **49**, 81–115.

Hessler AM, Lowe DR, Jones RL, Bird DK (2004) A lower limit for atmospheric carbon dioxide levels 3.2 billion years ago. *Nature* **428**, 736–738.

Hinrichs KU (2002) Microbial fixation of methane carbon at 2.7 Ga: was an anaerobic mechanism possible? *Geochemistry, Geophysics, Geosystems* **3**, doi: 10.1029/2001GC000286.

IPCC (2007) Climate change 2007: the physical science basis. In: *Contribution of Working Group I to the Fourth Assessment Report of the Intergovernmental Panel on Climate Change*. IPCC, Geneva, 996pp.

Kah LC, Riding R (2007) Mesoproterozoic carbon dioxide levels inferred from calcified cyanobacteria. *Geology* **35**(9), 799–802.

Karhu JA, Holland HD (1996) Carbon isotopes and the rise of atmospheric oxygen. *Geology* **24**(10), 867–870.

Kaufman AJ, Knoll AH (1995) Neoproterozoic variations in the C-isotopic composition of seawater: stratigraphic and biogeochemical implications. *Precambrian Research* **73**, 27–49.

Kaufman AJ, Xiao S (2003) High CO_2 levels in the Proterozoic atmosphere estimated from analyses of individual microfossils. *Nature* **20**, 121–148.

Kemp AIS, Hawkesworth CJ (2005) Granitic perspectives on the generation and secular evolution of the continental crust. In: *The Crust*, Vol. 3 (ed Rudnick RL), *Treatise on Geochemistry* (eds Holland HD, Turekian KK). Elsevier-Pergamon, Oxford, pp. 349–410.

Kleypas JA (1997) Modeled estimates of global reef habitat and carbonate production since the last glacial maximum. *Paleoceanography* **12**(4), 533–545.

Knoll AH (1991) End of the Proterozoic Eon. *Scientific American* **265**, 64–73.

Kump LR, Arthur MA (1999) Interpreting carbon-isotope excursions: carbonates and organic matter. *Chemical Geology* **161**(1–3), 181–198.

Kyser TK (1986) Stable isotope variations in the mantle. Stable isotope variations in high temperature geological processes. *Reviews of Mineralogy* **16**, 141–164.

Lasaga A, Ohmoto H (2002) The oxygen geochemical cycle: dynamics and stability. *Geochimica et Cosmochimica Acta* **66**(3), 361–381.

Lerman A, Wu L, Mackenzie FT (2007) CO_2 and H_2SO_4 consumption in weathering and material transport to the ocean, and their role in the global carbon cycle. *Marine Chemistry* **106**, 326–350.

Lowell RP, Keller SM (2003) High-temperature seafloor hydrothermal circulation over geologic time and Archean banded iron formations. *Geophysical Research Letters* **30**(7), doi: 10.1029/2002GL016536.

Ludwig W, Amiotte-Suchet P, Probst J-L (1999) Enhanced chemical weathering of rocks during the last glacial maximum: a sink for atmospheric CO_2? *Chemical Geology* **159**, 147–161.

Maher K, DePaolo DJ, Lin JC-F (2004) Rates of silicate dissolution in deep-sea sediment: in situ measurement using $^{234}U/^{238}U$ of pore fluids. *Geochimica et Cosmochimica Acta* **68**(22), 4629–4648.

Mann EM, Bradley RS, Hughes K (1998) Global-scale temperature patters and climate forcing over the past six centuries. *Nature* **392**, 779–787.

Marty B, Tolstikhin IN (1998) CO_2 fluxes from mid-ocean ridges, arcs and plumes. *Chemical Geology* **145**, 233–248.

Matsumoto R (1989) Isotopically heavy oxygen-containing siderite derived from the decomposition of methane hydrate. *Geology* **17**, 707–710.

Mattey DP (1987) Carbon isotopes in the mantle. *Terra Cognita* **7**, 31–37.

McElwain JC, Chaloner WG (1995) Stomatal density and index of fossil plants track atmospheric carbon dioxide in the Palaeozoic. *Annals of Botany* **76**, 389–395.

Melezhik VA, Fallick AE, Medvedev PV, Makarikhin VV (1999) Extreme $^{13}C_{carb}$ enrichment in ca. 2.0 Ga magnesite-stromatolite-dolomite-'red beds' association on a global context: a case for the world-wide signal enhanced by local environment. *Earth Science Reviews* **48**, 71–120.

Middelburg JJ (1989) A simple model for organic matter decomposition in marine sediments. *Geochimica et Cosmochimica Acta* **53**, 1577–1581.

Middelburg JJ, Vlug T, van der Nat FJWA (1993) Organic matter mineralization in marine systems. *Global and Planetary Change* **8**, 47–58.

Munhoven G (2002) Glacial-interglacial changes of continental weathering: estimates of the related CO_2 and HCO_3^- flux variations and their uncertainties. *Global and Planetary Change* **33**, 155–176.

Nakamura K, Kato Y (2002) Carbonate minerals in the Warrawoona Group, Pilbara Craton: Implications for continental crust, life, and global carbon cycle in the Early Archean. *Resource Geology* **52**(2), 91–100.

Pagani M, Arthur MA, Freeman KH (1999a) Miocene evolution of atmospheric carbon dioxide. *Paleoceanography* **14**, 273–292.

Pagani M, Freeman KH, Arthur MA (1999b) Late Miocene atmospheric CO_2 concentrations and the expansion of C4 grasses. *Science* **285**, 876–879.

Pavlov AA, Kasting JF, Eigenbrode JL, Freeman KH (2001) Organic haze in Earth's early atmosphere: source of low-C-13 Late Archean kerogens? *Geology* **29**(11), 1003–1006.

Pearson PN, Palmer MR (2000) Atmospheric carbon dioxide concentrations over the past 60 million years. *Nature* **406**, 695–699.

Pearson DG, Canil D, Shirey SB (2004) Mantle samples included in volcanic rocks: xenoliths and diamonds. In: *Treatise on Geochemistry*, Vol. 2 (eds H.D. Holland HD, Turekian KK). Elsevier, Oxford, pp. 172–221.

Petit JR, Jouzel J, Raynaud D, *et al*. (1999) Climate and atmospheric history of the past 420,000 years from the Vostok ice core, Antarctica. *Nature* **399**(6735), 429–436.

Petsch ST, Eglinton TI, Edwards KJ (2001) 14C-dead living biomass: evidence for microbial assimilation of ancient organic carbon during shale weathering. *Science* **292**, 1127–1131.

Prokoph A, Shields GA, Veizer J (2008) Compilation and time-series analysis of a marine carbonate &sbull;^{18}O, &sbull;^{13}C, $^{87}Sr/^{86}Sr$ and &sbull;^{34}S database through Earth history. *Earth-Science Reviews* **87**, 113–133.

Raymo ME (1994) The Himalayas, organic carbon burial, and climate in the Miocene. *Paleoceanography* **9**(3), 399–404.

Resing JA, Lupton JE, Feely RA, Lilley MD (2004) CO_2 and ^3He in hydrothermal plumes: implications for mid-ocean ridge CO_2 flux. *Earth and Planetary Science Letters* **226**, 449–464.

Rey PF, Coltice N (2008) Neoarchean lithospheric strengthening and the coupling of the Earth's geochemical reservoirs. *Earth and Planetary Science Letters* **36**(8), 635–638

Ridgwell A, Hargreaves JC (2007) Regulation of atmospheric CO_2 by deep-sea sediments in an Earth system model. *Global Biogeochemical Cycles* **21**(2), GB2008.

Riebesell U, Schulz KG, Bellerby RGJ, *et al*. (2007) Enhanced biological carbon consumption in a high CO_2 ocean. *Nature* **450**, 545-U10.

Rothman DH, Hayes JM, Summons, RE (2003) Dynamics of the Neoproterozoic carbon cycle. *Proceedings of the National Academy of Sciences,USA* **100**, 8124-8129.

Royer DL (2006) CO_2-forced climate thresholds during the Phanerozoic. *Geochimica et Cosmochimica Acta* **70**, 5665–5675.

Royer DL, Berner RA, Park J (2007) Climate sensitivity constrained by CO_2 concentrations over the past 420 million years. *Nature* **446**, 530–532.

Rundgren M, Beerling D (1999) A Holocene CO_2 record from the stomatal index of sub-fossil *Salix herbacea* L. leaves from northern Sweden. *Holocene* **9**, 509–513.

Rye R, Kuo PH, Holland HD (1995) Atmospheric carbon dioxide concentrations before 2.2 billion years ago. *Nature* **378**, 603–605.

Sano Y, Williams SN (1996) Fluxes of mantle and subducted carbon along convergent plate boundaries. *Geophysical Research Letters* **23**(20), 2749–2752.

Sarmiento JL, Gruber N (2006) *Ocean Biogeochemical Cycles*. Princeton University Press, Princeton, NJ.

Sheldon ND (2006) Precambrian paleosols and atmospheric CO_2 levels. *Precambrian Research* **147**, 148–155.

Seward TM, Kerrick DM (1996) Hydrothermal CO_2 emission from the Taupo Volcanic Zone, New Zealand. *Earth and Planetary Science Letters* **139**, 105–113.

Shields GA (2007) A normalised seawater strontium isotope curve and the Neoproterozoic-Cambrian chemical weathering event. *eEarth Discussions* **2**(69–84).

Sleep NH, Zahnle K (2001) Carbon dioxide cycling and implications for climate on ancient Earth. *Journal of Geophysical Research-Planets* **106**(E1), 1373–1399.

Strauss H, Moore TB (1992) Abundances and isotopic compositions of carbon and sulfur species in whole rock and kerogen samples. In: *The Proterozoic Biosphere* (eds Schopf JW, Klein C). Cambridge University Press, Cambridge, pp. 709–798.

Syvitski J P M, Vorosmarty C.J, Kettner A J, Green P. (2005) Impact of humans on the flux of terrestrial sediment to the global coastal ocean. *Science* **308**(5720), 376-380.

Teagle DAH, Alt JC, Bach W, Halliday AN, Erzinger J (1996) Alteration of upper ocean crust in a ridge-flank hydrothermal upflow zone: mineral, chemical and isotopic constraints from hole 896A. *Proceedings of the Ocean Drilling Program, Scientific Results* **148**, 119–150.

Van der Burgh J, Visscher H, Dilcher DL, Kürschner WM (1993) Paleoatmospheric signatures in Neogene fossil leaves. *Science* **260**, 1788–1790.

Veizer J (1989) Strontium isotopes in seawater through time. *Annual Review of Earth and Planetary Sciences* **17**, 141–167.

Veizer J, Compston W (1974) $^{87}Sr/^{86}Sr$ composition of seawater during the Phanerozoic. *Geochimica et Cosmochimica Acta* **38**, 1461–1484.

Veizer J, Compston W (1976) Sr-87–Sr-86 in Precambrian carbonates as an index of crustal evolution. *Geochimica et Cosmochimica Acta* **40**(8), 905–914.

Veizer J, Laznicka P, Jansen SL (1989) Mineralization through geologic time: recycling perspective. *American Journal of Science* **289**, 484–524.

Walker JCG (1990) Precambrian evolution of the climate system. *Global and Planetary Change* **82**(3–4), 261–289.

Walker JCG, Hays PB, Kasting JF (1981) A negative feedback mechanism for the long-term stabilization of Earth's surface temperature. *Journal of Geophysical Research* **86**, 9776–9782.

Wallmann K (2001) Controls on Cretaceous and Cenozoic evolution of seawater composition, atmospheric CO_2 and climate. *Geochimica et Cosmochimica Acta* **65**(18), 3005–3025.

Wallmann K (2004) Impact of atmospheric CO_2 and galactic cosmic radiation on Phanerozoic climate change and the marine &sbull;^{18}O record. *Geochemistry, Geophysics, Geosystems* **5**(1), doi:10.1029/2003GC000683.

Wallmann K, Aloisi G, Haeckel M, Obzhirov A, Pavlova G, Tishchenko P (2006) Kinetics of organic matter degradation, microbial methane generation, and gas hydrate formation in anoxic marine sediments. *Geochimica et Cosmochimica Acta* **70**, 3905–3927.

Wallmann K, Aloisi G, Haeckel M, *et al*. (2008) Silicate weathering in anoxic marine sediments. *Geochimica et Cosmochimica Acta* **72**, 3067–3090.

Zachos JC, Pagani M, Sloan L, Thomas E, Billups K (2001) Trends, rhythms, and aberrations in global climate 65 Ma to present. *Science* **292**, 686–693.